Fabrication of fucoxanthin/2-hydroxypropyl-β-cyclodextrin inclusion complex assisted by ultrasound procedure to enhance aqueous solubility, stability and antitumor effect of fucoxanthin

Xiaowen Sun [a,b], Junxiang Zhu [c], Chengqin Liu [d], Dongfeng Wang [a], Chang-Yun Wang [a,b,*]

[a] *Key Laboratory of Marine Drugs, The Ministry of Education of China, School of Medicine and Pharmacy, College of Food Science and Engineering, Ocean University of China, Qingdao 266003, Shandong, China*
[b] *Laboratory for Marine Drugs and Bioproducts, Qingdao National Laboratory for Marine Science and Technology, Qingdao 266237, Shandong, China*
[c] *College of Food Science and Engineering, Qingdao Agricultural University, Qingdao 266109, Shandong, China*
[d] *Department of Cardiology, Binzhou Medical University Hospital, Binzhou 256699, Shandong, China*

ARTICLE INFO

ABSTRACT

Fucoxanthin (Fx) possesses multiple bioactivities such as antitumor, antioxidant and anti-inflammatory activities, but its application is limited due to the poor water solubility, low bioavailability, and instability to some external harsh conditions. In this study, a stable inclusion complex of Fx and 2-hydroxypropyl-β-cyclodextrin (2-HP-β-CD) was prepared with the aid of ultrasound, which was characterized by scanning electron microscope, Fourier transform infrared spectroscopy, powder X-ray diffraction, and differential scanning calorimetry techniques. The phase solubility analysis and absorption spectroscopy results showed that Fx formed stoichiometry 1:2 inclusion complex with 2-HP-β-CD, and this could be well proved by molecular simulation. Structural analyses and molecular docking study indicated that Fx was successfully encapsulated into the cavity of 2-HP-β-CD, promoting it soluble in water and stable against heat, storage and gastrointestinal environments. In addition, Fx/2-HP-β-CD inclusion complex exhibited excellent antitumor activity against HCT116 and Caco-2 cell lines with IC_{50} values of 12.0 μM and 14.86 μM, respectively. Therefore, it could be a potentially promising way to promote the application of Fx in pharmaceuticals and functional foods by HP-β-CD encapsulation strategy.

1. Introduction

Fucoxanthin (Fx) is the most abundant carotenoid in the nature, contributing more than 10 % of estimated total natural carotenoids [1]. It is widely present in brown algae such as *Undaria pinnatifida* and *Sargassum fusiforme*, which have been used as food and materia medica in China with a long history. As a natural dietary supplement, Fx encompasses multiple bioactivities such as antioxidant, anti-obesity, anti-inflammatory, antitumor and anti-diabetic properties [2–5]. Fx has a unique structure including an allenic bond, an epoxide group, and a conjugated carbonyl group in the polyene chain. Owing to the highly unsaturated structure, Fx is water insoluble and extremely susceptible to oxygen, heat and gastrointestinal environment, which limit its bioavailability as well as health efficacy to a great extent [6,7].

β-Cyclodextrin (β-CD), a cyclic oligosaccharide consisting of seven glucose units connected by α-1,4-glycosidic bond, has been widely used to improve the stability and water solubility of various guest molecules in the form of host–guest inclusion complexes [8–11]. However, native β-CD is encountered with the relatively low aqueous solubility and hemolytic effects [12,13], limiting its pharmaceutical and nutrition supplemental application. To overcome these drawbacks, 2-hydroxypropyl-β-cyclodextrin (2-HP-β-CD) was proposed and designed, which has been listed in European Pharmacopoeia and US Pharmacopoeia [14,15]. The available literatures show that 2-HP-β-CD displays high solubility in water, relatively large inclusion capacity and low toxicity *in vivo*, which is more suitable for oral or intravenous administration. As a result, 2-HP-β-CD has attracted more and more attention of researchers to investigate its use in drug delivery [16–18].

Ligand–CD inclusion complexes are mostly formed via weak non-covalent interactions such as hydrogen bonding and electrostatic

attraction. Nevertheless, a relatively long reaction time will be needed if let the complexation reaction happen spontaneously. Actually, ultrasonication is a relatively cheaper and ecofriendly green technology, which can effectively provide energy to facilitate the formation of CD-based inclusion complexes and improve the properties of lipophilic bioactive components. In our previous study, we prepared 2-HP-β-CD embedded Fx microcapsule using Tween 80 as emulsifying agent with the help of ultrasonication (500 W, 10 min) and spray drying [19]. Cui and colleagues prepared the inclusion complex of cuminaldehyde with 2-HP-β-CD assisted by ultrasonic waves at 60 W for 30 min, effectively improving the aqueous solubility, thermal stability as well as antibacterial activities of cuminaldehyde [20]. Jiang et al. prepared tea tree oil/HP-β-CD inclusion complex via the ultrasonic wave of 120 W at 40 °C for 70 min, and found that the stability and long-lasting antifungal properties were improved [16]. Compared with the surfactant- or emulsion-based delivery systems, CD-based inclusion complexes based on molecular recognition has the characteristics of high safety, low energy consumption and easy preparation.

In this work, a novel inclusion complex of Fx and 2-HP-β-CD was fabricated with the aid of ultrasonic waves. The stoichiometry parameter and association constant of guest/host in the Fx/2-HP-β-CD inclusion complex (Fx/2-HP-β-CD IC) were investigated by analyzing the phase solubility and UV–Vis absorption spectra of Fx in 2-HP-β-CD solutions with different concentrations. The Fx/2-HP-β-CD IC was subsequently characterized using Fourier transform infrared spectroscopy (FT-IR), powder X-ray diffraction (PXRD), differential scanning calorimetry (DSC), and scanning electron microscope (SEM). Finally, the solubilization, chemical stability and antitumor activities of Fx/2-HP-β-CD IC were investigated.

2. Materials and methods

2.1. Materials

Fucoxanthin (Fx, 98 %) was purchased from sigma-Aldrich (St. Louis, MO, USA), and 2-HP-β-CD (≥99.5 %) from Macklin Biochemical Co., ltd (Shanghai, China). Absolute alcohol and potassium bromide (KBr, spectroscopic grade) were provided by Sinopharm Chemical Reagent Co., Ltd (Shanghai, China). The advanced DMEM medium, FBS, penicillin–streptomycin solution (100×) and 0.25 % trypsin-0.04 % EDTA were supplied by Biological Industries (Kibbutz Beit Haemek, Israel). Water used in the experiments was prepared by a Milli-Q system (Millipore Corporation, USA). All the other chemicals used were of analytical grade.

2.2. Phase solubility measurements

Phase solubility analysis of Fx in 2-HP-β-CD solutions was performed according to the method reported by Higuchi and Connors [21]. Excess amounts of Fx (10 mg) were added to the aqueous solutions of 2-HP-β-CD at various concentrations (0–175 mM). The premixtures were treated by ultrasonic wave for 30 min and then shaken on thermostatic oscillators at 303 K for 72 h. After equilibrium was achieved, 2 mL of each solution was filtered through a 0.45 μm PES micro filter, properly diluted, and finally analyzed using an ultraviolet–visible (UV–Vis) spectrophotometer (UV-2800 Unico Instrument Co., ltd., Shanghai, China) at 460 nm. The concentrations of Fx in solutions were calculated according to the standard curve. The phase solubility curve was plotted with 2-HP-β-CD concentrations on the x-axis and Fx concentrations on the y-axis.

2.3. UV–Vis absorption spectroscopy and thermodynamic analysis

The UV–Vis absorption spectra of Fx in 2-HP-β-CD solutions with various concentrations were measured with a UV-2800 spectrophotometer from 280 nm to 600 nm. The concentration of Fx was kept at

50 μM. The absorption values at 460 nm of Fx were used to calculate the stoichiometry and association constants (K_a) of Fx/2-HP-β-CD IC. The Benesi-Hildebrand (B-H) double reciprocal method was exploited to determine the stoichiometry of Fx/2-HP-β-CD IC via the equation (1) and (2) [22].

$$\frac{1}{A - A_0} = \frac{1}{(A' - A_0) K_a \left[2 - HP - \beta - CD \right]} + \frac{1}{A' - A_0} \tag{1}$$

$$\frac{1}{A - A_0} = \frac{1}{(A' - A_0) K_a \left[2 - HP - \beta - CD \right]^2} + \frac{1}{A' - A_0} \tag{2}$$

Where A and A_0 are the absorption values of Fx in the presence and absence of 2-HP-β-CD, A' represents the absorption value of Fx at the maximum concentration of 2-HP-β-CD. [2-HP-β-CD] is the concentration of 2-HP-β-CD in the solution.

2.4. Preparation of Fx/2-HP-β-CD IC

The inclusion complex was prepared assisted by ultrasound procedure with some modification [20]. Firstly, 2-HP-β-CD was dissolved in 75 % ethanol at concentration of 15 mM and Fx was dissolved in 75 % ethanol at 0.5 mM. Both the stock solutions were filtered to remove insoluble substance. Then the Fx soulution was added dropwise to 2-HP-β-CD solution at the molar ratio of Fx to 2-HP-β-CD as 1:25. The mixed solution was blended thoroughly with a vortex for 5 min. Subsequently, the rough mixture was treated using an ultrasonic homogenizer (Scientz-IID, China) at 60 W for 30 min with a duty ratio of 60 % and then gone through a gentle magnetic stirring at 30 °C for 24 h. The ethanol was removed in vacuo and adequate water was added to replenish the lost volume. The dispersion was filtered and then lyophilized to obtain solid Fx/2-HP-β-CD IC.

2.5. Scanning electron microscopy (SEM)

Small amount of powder sample of Fx, 2-HP-β-CD, or Fx/2-HP-β-CD IC was evenly distributed on double-sided copper tape and fixed on an aluminium stub. The sample was made electrically conductive by sputter-coating a thin layer of gold and placed inside the specimen chamber of SEM. SEM photographs were obtained using a Regulus 8100 FE-SEM system (Hitachi, Japan) at an accelerating voltage of 5.0 kV. The obtained SEM micrographs were examined for characterization of the morphology of the various microparticles.

2.6. Complexation efficiency of Fx in Fx/2-HP-β-CD IC

An accurately amounts (10 mg) of Fx/2-HP-β-CD IC was weighted and dissolved completely in methanol and sonicated for 30 min to allow all Fx dissolved into solution. Then, the mixture was centrifuged (5000 rpm, 30 min) to collect the supernatant rich in Fx. The content of Fx encapsulated was measured using an UV–Vis spectrophotometer. The sample was prepared and analyzed in triplicate. The complexation efficiency (*CE*) was calculated using the following equation [23].

$$CE = \frac{M}{M_0} \times 100\% \tag{3}$$

where M is the content of encapsulated Fx, and M_0 is the initial content of Fx added.

2.7. Fourier-transform infrared spectroscopy (FT-IR)

FT-IR spectra of Fx, 2-HP-β-CD, and Fx/2-HP-β-CD IC were obtained by the KBr tablets method using a Nicolet iS10 spectrophotometer (Thermo Fisher Scientific, Waltham, MA, USA) in room temperature. All the spectra were obtained over a continuous frequency range of 4000–400 cm^{-1}.
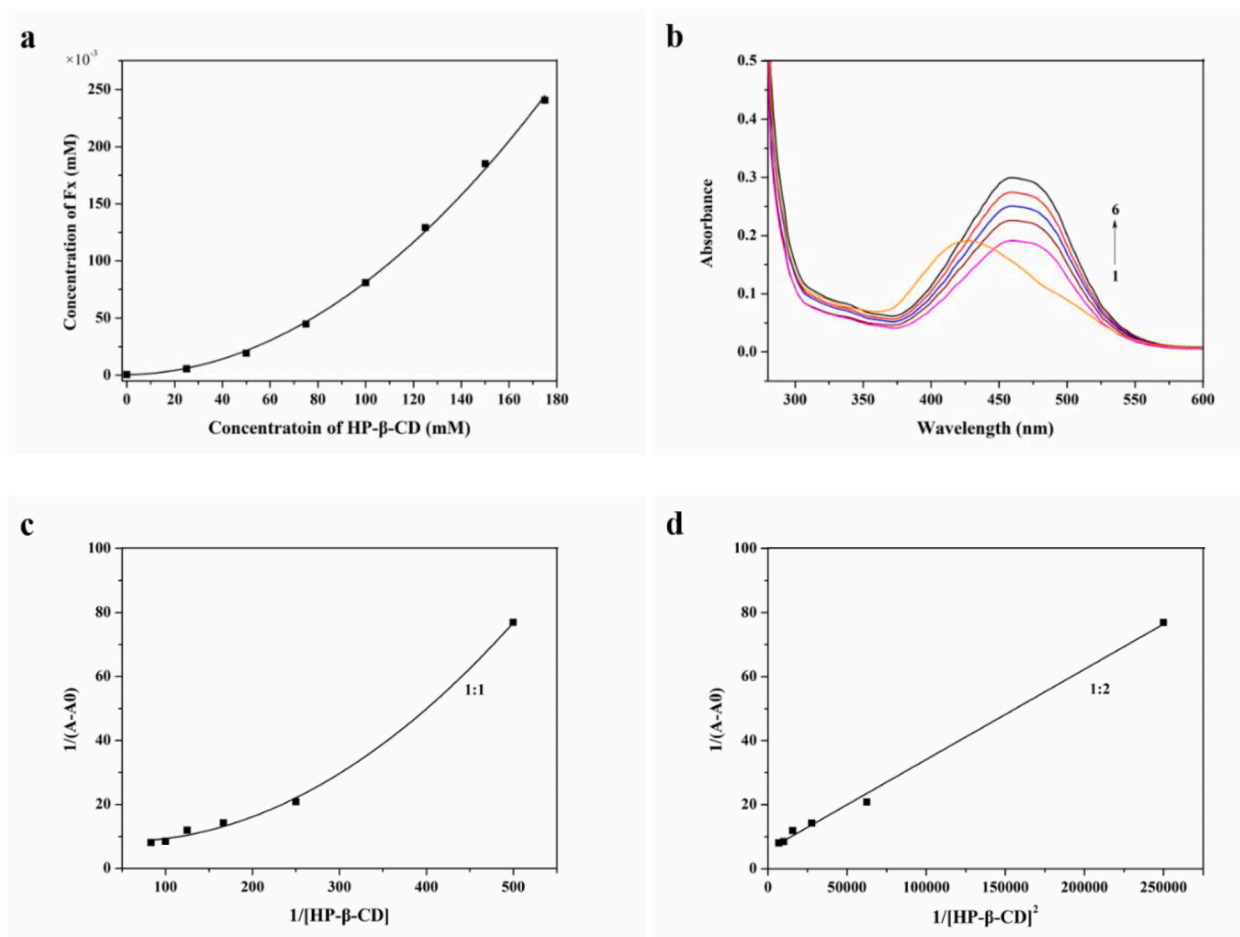
Fig. 1. Stoichiometry characteristics of Fx/2-HP-β-CD IC. (a) Phase solubility plot of Fx/2-HP-β-CD IC system; (b) Absorption spectra of Fx (5×10^{-5} M) in aqueous solutions with various concentrations of 2-HP-β-CD (1) 0, (2) 0.002, (3) 0.004, (4) 0.006, (5) 0.008, and (6) 0.01 M; (c) The corresponding Benesi-Hildebrand plot of $1/(A-A_0)$ versus $1/[2\text{-HP-}\beta\text{-CD}]$ and (d) $1/(A-A_0)$ versus $1/[2\text{-HP-}\beta\text{-CD}]^2$ for the complexation between Fx and 2-HP-β-CD.

2.8. Powder X-ray diffraction (XRD)

Monochromatic Cu Ka radiation (wavelength = 1.54056 Å) was produced by a Bruker D8 Advance diffractometer (Bruker, Germany). The powder sample was well ground and packed tightly in a rectangular aluminum cell prior to exposure to the X-ray beam. Scanning region of the diffraction angle, 2θ, was set at 5–40° and radiation was detected with a proportional detector.

2.9. Thermal characteristic analysis

Around 5 mg of sample in aluminum crucible was measured using a DSC 200 PC (NETZSCH, Germany) instrument in a dynamic nitrogen atmosphere with a flow rate of 50 mL/min. The heat rate was 10 °C/min and the temperature ranged from 40 °C to 300 °C.

2.10. Molecular docking

The crystal structure of β-CD (entry code 1DMB) was extracted from the Protein Data Bank (https://www.rcsb.org). The structure of 2-HP-β-CD was constructed by incorporating hydroxypropyl into β-CD and energy minimized using Avogadro molecular editor. The crystal structure of Fx was obtained from the Zinc database (entry code ZINC71318645) and its structural energy minimization was also performed with Avogadro molecular editor. Docking between 2-HP-β-CD and Fx was performed using the AutoDock 4.2 program in a grid box covering the entire system. The possible 2-HP-β-CD-Fx conformations were ascertained using Lamarckian genetic algorithm (LGA) and visualized using the PyMOL (version 2.3.2). The binding energy ($\Delta G_{\text{binding}}$) was calculated using the following equation [7].

$$\Delta G_{binding} = \Delta G_{vdW+Hbond+desolv} + \Delta G_{elec} + \Delta G_{intern} + \Delta G_{tor} - \Delta G_{unb} \quad (4)$$

where, $\Delta G_{\text{vdW+Hbond+desolv}}$ is the sum of the van der Waals, hydrogen bonding and desolvation energy. ΔG_{elec} is the electrostatic energy, ΔG_{intern} is the total internal energy, ΔG_{tor} is the torsional free energy, and ΔG_{unb} is the uound system's energy.

2.11. Solubilization test

Solubility studies were done following similar procedures reported previously [24]. Excess quantity of Fx (10 mg) or Fx/2-HP-β-CD IC (300 mg) was respectively added into certain amount of distilled water (1 mL) to obtain supersaturated solution. Both the solutions were continuously stirred at 25 °C for 24 h to ensure the equilibrium states were achieved. Then, each solution was filtered through a 0.45 μm PES micro filter, and detected using UV–Vis method to calculate the dissolved content of Fx.

2.12. Heat, Storage, and gastrointestinal stability of Fx/2-HP-β-CD IC

The chemical stability of Fx/2-HP-β-CD IC was evaluated by exposing the samples to a series of simulated processing and storage stage or simulated internal environmental conditions. The Fx/2-HP-β-CD IC was dissolved in PBS with final Fx concentration of 40 μM hold at 65 °C for
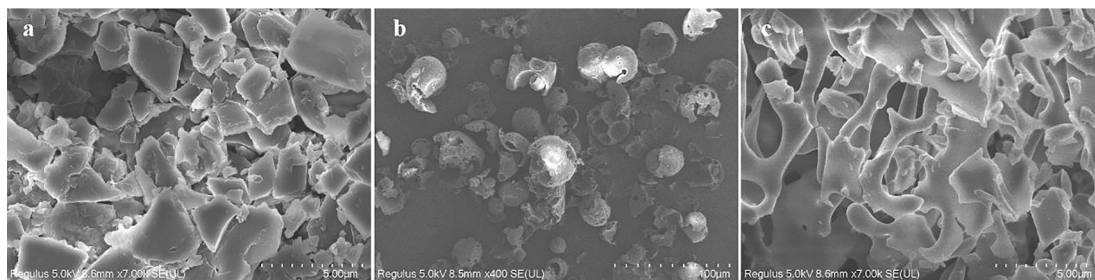
Fig. 2. Scanning electron microscope images of (a) Fx, (b) 2-HP-β-CD, (c) Fx/2-HP-β-CD IC.

30 min to measure its heat stability. The storage stability of Fx/2-HP-β-CD IC was measured during the sample kept at 25 °C in darkness (0–20 d). The simulated internal environmental stability of Fx/2-HP-β-CD IC was assessed by exposing the samples to a range of simulating physiological conditions: gastric juice (pH = 2.0 HCl), small intestinal juice (pH = 7.4 PBS), and normal saline solution (0.9 % NaCl, w/v), all the systems were maintained at 37 °C to simulate body temperature. For all the stability tests, periodic sampling was conducted and the amount of Fx remaining was detected. All experiments were performed in triplicate. The retention index (*RI*) of Fx was calculated using equation (5).

$$RI\ (\%) \ = \ \frac{C}{C_0} \times 100 \tag{5}$$

Where C is the remaining amount of Fx, and C_0 is the initial amount of Fx.

2.13. Antiproliferative activity assay

Human colonic adenocarcinoma HCT116 and Caco-2 cells were cultured in the advanced DMEM containing 10 % (v/v) of FBS, and 1 % penicillin–streptomycin solution, and maintained at 37 °C under 5 % CO_2 humidified atmosphere. Cell viability was measured using MTT assay method. HCT116 and Caco2 cells were inoculated in 96-well plates at a density of 2×10^4 per well. After incubated for 12 h, the cells were treated with free Fx (dissolved in DMSO with a final working concentration of <0.1 %), 2-HP-β-CD or Fx/2-HP-β-CD IC (dissolved in PBS) at corresponding concentrations. After 24 h incubation, the medium was replaced with 100 μL fresh DMEM containing 10 % MTT solution and incubated for 4 h. The medium was then removed and 110 μL of DMSO was added into each well to dissolve the formazan crystals. The absorbance at 570 nm was measured using a VICTOR Nivo multimode plate reader (PerkinElmer, USA). DMEM medium was used as the negative control group. The cell viability (*CV*) was calculated according to the following formula:

$$CV\ (\%) \ = \ \frac{A_1 - A_0}{A' - A_0} \times 100 \tag{6}$$

where A_1, A' and A_0 are the absorption values of experimental well, negative control well and blank well.

2.14. Statistical analysis

All the data were expressed as the mean ± standard deviation (SD). Statistical analysis was performed using one-way ANOVA in SPSS 19.0 software (SPSS Inc., Chicago, IL, USA), followed by the post-hoc Tukey's test.

3. Results and discussion

3.1. Stoichiometry study for Fx/2-HP-β-CD IC

3.1.1. Phase solubility study

Phase solubility method is widely used to evaluate the inclusion capability of cyclodextrins to entrap guest molecules and stoichiometry of the inclusion complex [25]. In this study, the dynamic equilibrium of Fx/2-HP-β-CD system was reached up to 72 h at 303 K and then the absorbances of Fx in filtrated solutions were measured at 460 nm. Fig. 1a showed the phase solubility plot of Fx at diverse concentrations of 2-HP-β-CD, which exhibited a positive curvature. Based on Higuchi and Connors's theory, it was classified as A_P type phase solubility diagram, indicating that a inclusion complex with stoichiometric ratio of 1:2 was formed between Fx and 2-HP-β-CD [21,25]. The solubility of Fx was apparently enhanced as the concentrations of 2-HP-β-CD increased.

3.1.2. UV–Vis spectra analysis

The UV–Vis absorption spectra of Fx (50 μM) in aqueous solutions of 2-HP-β-CD with gradient-varying concentrations (0–0.01 M) were examined. The absorption spectra of Fx in aqueous solutions without and with 2-HP-β-CD were shown in Fig. 1b. In general, the addition of 2-HP-β-CD significantly caused a spectral shift and increased the absorption intensity of Fx. From 300 nm to 600 nm, the absorption spectrum of Fx possessed a maximum absorption at 428 nm in aqueous solution, which was attributed to Fx forming H-aggregates in water [26]. The addition of 2-HP-β-CD caused a prominent bathochromic shift of up to 32 nm. In addition, the absorption at 460 nm increased gradually as the concentrations of 2-HP-β-CD increased. The above-mentioned spectral changes confirmed that Fx was entrapped into 2-HP-β-CD and formed inclusion complex. It was speculated that the enhancement of the dissolution of Fx may be attributed to the hydrophobic interaction between Fx and non-polar cavity of 2-HP-β-CD [20].

The Benesi-Hildebrand double reciprocal method is conducive to confirm the stoichiometry and kinetic parameters involved in the process of inclusion complex formation [27]. Here, the dependency-relationship between Fx absorbances and 2-HP-β-CD concentrations was analyzed using B-H double reciprocal method. Fig. 1c and 1d showed the B-H plots for Fx/2-HP-β-CD IC with stoichiometric ratios of 1:1 and 1:2, respectively. The plot of $1/(A - A_0)$ vs $1/[2\text{-HP-}\beta\text{-CD}]$ appeared an upward curve (Fig. 1c). While a good linear correlation with a correlation coefficient $R^2 = 0.9963$ was obtained by Eq. (2) (Fig. 1d), which supported that an inclusion complex was formed between Fx and 2-HP-β-CD with a ratio of 1:2. Therefore, the Fx/2-HP-β-CD IC was characterized with a stoichiometric ratio of 1:2 which was co-proved by the phase solubility diagram and B-H linear-regression plot. The K_a value for the Fx/2-HP-β-CD IC formation was calculated to be $2.08 \times 10^4 \ M^{-2}$.

3.2. Structural characterization of Fx/2-HP-β-CD IC

3.2.1. Scanning electron microscopy (SEM) analysis

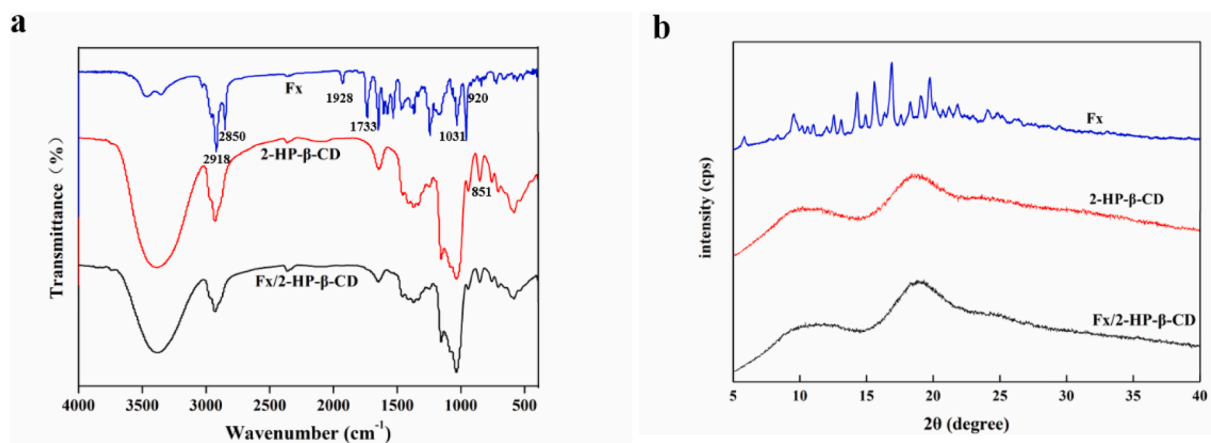SEM can be employed for investigating the surface morphology and

Fig. 3. The FT-IR spectra (a) and powder XRD patterns (b) of Fx, 2-HP-β-CD and Fx/2-HP-β-CD IC.

microstructural properties of the guest molecules with or without complexing with cyclodextrins. As shown in Fig. 2a, free Fx appeared as sheets with smooth surface. Single 2-HP-β-CD particles were in the forms of spherical shapes with cavity structures (Fig. 2b). Whereas, the Fx/2-HP-β-CD IC presented as irregularly rodlike structures and the initial morphologies of Fx and 2-HP-β-CD vanished (Fig. 2c). Besides the shape differentiation, the size of the solid complex was also different from those of Fx and 2-HP-β-CD. These changes also indicated that the Fx/2-HP-β-CD IC was indeed formed. The complexation efficiency of inclusion complex was further determined as 92.70 % by measuring UV–Vis absorption values and calculating with the equation (3).

3.2.2. FT-IR analysis

FT-IR analysis was performed to evaluate the interaction between Fx and 2-HP-β-CD in the inclusion complex. The FT-IR spectra of 2-HP-β-CD, free Fx, and Fx/2-HP-β-CD IC were presented in Fig. 3a. The band at 851 cm^{-1} was characteristic for the C—O—C skeletal mode of α-glycosidic linkage in 2-HP-β-CD structure [28]. In the FT-IR spectrum of free Fx, the characteristic ester carbonyl (C=O) stretching vibration band was found at 1733 cm^{-1}. The band at 1031 cm^{-1} was assigned to the telescopic vibration of C—O ester. The band at 1928 cm^{-1} was assigned to the allenic bond (C=C=C), a distinctive functional group of Fx [29]. The peaks at 2918 cm^{-1} and 2850 cm^{-1} were attributed to the alkanes with C — H bonds. And the peak at 920 cm^{-1} reflected the presence of the epoxy group. Whereas, the major peaks of Fx disappeared in the IR spectrum of Fx/2-HP-β-CD IC. Synthesizing all the FT-IR results, it could be deduced that Fx was successfully entrapped by the hydrophobic cavity of 2-HP-β-CD and inclusion complex was formed, which led to the characterized functional groups of Fx were shielded.

3.2.3. XRD analysis

XRD analysis is an efficient means to investigate the complexation process of guest molecules and cyclodextrins. XRD analyses of Fx, 2-HP-β-CD, and Fx/2-HP-β-CD IC were conducted and shown in Fig. 3b. Fx displayed sharp and intense peaks, which clearly indicated crystal morphologies. While, there was a distinctive characteristic amorphous diffraction pattern with two broad band at 2θ ~ 10° and 18° in the XRD pattern of 2-HP-β-CD. Furthermore, the diffraction pattern of Fx/2-HP-β-CD IC showed amorphous structure as well. These results illustrated that Fx had been encapsulated by 2-HP-β-CD in an inclusion complex state, which were in agreement with the findings from FT-IR.

3.3. Thermal characteristic analysis of Fx/2-HP-β-CD IC

DSC analysis is a common technique that can be used in checking the complexation of guest molecules and host cyclodextrins by giving the thermodynamic information of samples against temperature/time. In
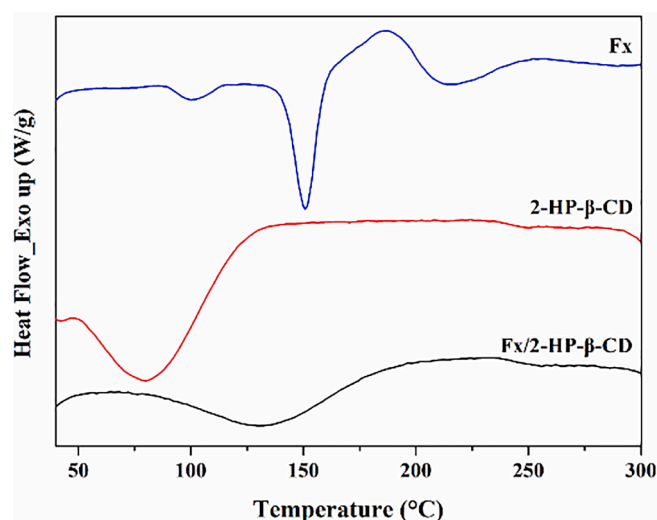

Fig. 4. DSC curves of Fx, 2-HP-β-CD, and Fx/2-HP-β-CD IC.

this study, DSC analyses of Fx, 2-HP-β-CD, and Fx/2-HP-β-CD IC were performed and shown in Fig. 4. The thermogram of Fx had a broad endotherm at 99 °C attributed to the release of water molecules, a sharp melting endotherm at 151 °C ascribed to the fusion point of Fx [30]. The thermal curve of 2-HP-β-CD displayed a broad endotherm around 80 °C relevant to the loss of crystal water from its cavity [31,32]. However, the characteristic melting peak of Fx absolutely disappeared in the DSC thermogram of Fx/2-HP-β-CD IC, which confirmed that Fx was embedded into the non-polar cavity of 2-HP-β-CD and hence formed an amorphous complex. It has been reported that there would be no crystalline guest structure to absorb energy if guest molecules had formed inclusion complex with cyclodextrins [33,34]. Whereas there was only a broad endotherm peak at 130 °C in DSC curve of Fx/2-HP-β-CD IC accompanied by significant decrease in the intensity, indicating the water loss from sample. It could be speculated that several water molecules contained in the cavity of 2-HP-β-CD were expelled to establish hydrogen bondings with Fx molecule, thus the energy dissipation in dehydration process increased [33,35]. Similar reduction in dehydration peaks was also observed in the formation of sulfadimethoxine/cyclodextrins complex [36]. The above results further confirmed that Fx had been complexed with 2-HP-β-CD.

3.4. Molecular docking

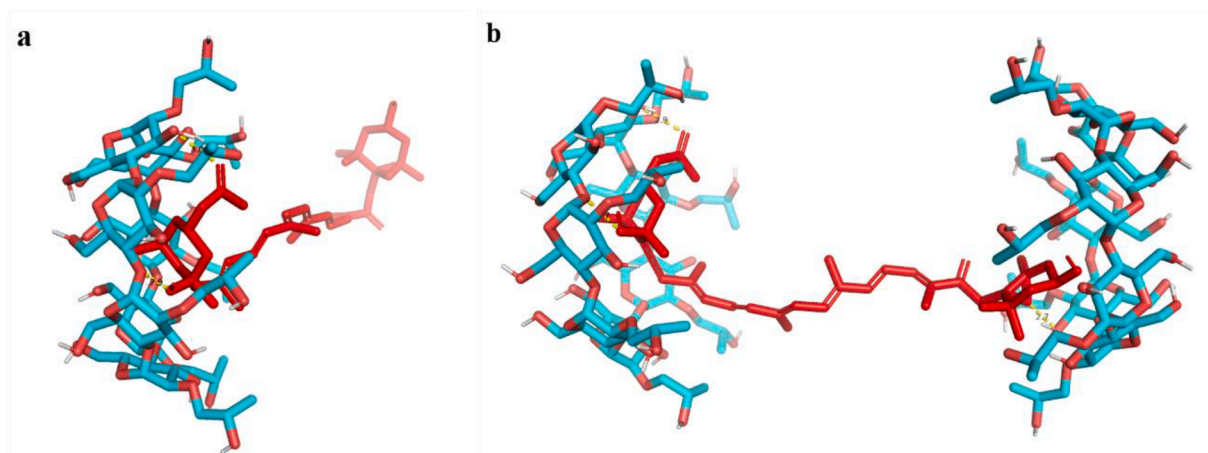Molecular docking *in silico* is an effective tool to rationally design the

Fig. 5. Optimized geometries obtained for inclusion complexes (a) 1:1 Fx/2-HP-β-CD IC and (b) 1:2 Fx/2-HP-β-CD IC. Yellow dotted lines represent the intermolecular hydrogen bonds between 2-HP-β-CD and Fx molecules.

Table 1
Molecular docking results of Fx/2-HP-β-CD combined modes.[a]

Mode	$\Delta G_{binding}$	$\Delta G_{vdW+hb+desolv}$	ΔG_{elec}	ΔG_{intern}	ΔG_{tor}	ΔG_{unb}
1:1Fx/2-HP-β-CD	−15.94	−34.35	−0.29	−9.29	18.70	−9.29
1:2Fx/2-HP-β-CD	−37.29	−55.96	−0.04	−6.78	18.71	−6.78

[a]Unit is kJ· mol^{-1};

drug delivery systems, which is helpful to better understand the molecular assembly and reliably predict the preferred conformation [7]. In order to authenticate the experimental results described above, we performed molecular docking studies using the Lamarckian genetic algorithm. According to the calculation results of phase solubility and Benesi-Hildebrand liner regression, the combination of Fx and 2-HP-β-CD was at a molar ratio of 1:2. The initial conformation of Fx was fully optimized in vacuum and docked with 2-HP-β-CD. Molecular simulation results also showed that Fx and 2-HP-β-CD molecules can form inclusion complexes. There were 100 alternative Fx/2-HP-β-CD conformations obtained for 1:1 and 1:2 guest/host ratio respectively. The optimal geometrical structures of Fx/2-HP-β-CD ICs with least binding energy were obtained, which were visualized using Pymol (version 2.1,

CA, USA) software and shown in Fig. 5. All the conformations indicated that the entire Fx molecule could not be wrapped totally in the cavity of 2-HP-β-CD for the long chain of Fx exceeds the depth of the cavity.

Table 1 summarized binding free energy of the possible modes. The results indicated that Fx could form a range of inclusion complexes with 2-HP-β-CD at varying negative $\Delta G_{binding}$, indicating further all modes were thermodynamically favorable. However, the optimal mode of Fx/2-HP-β-CD IC at molar ratio of 1:2 ($\Delta G_{binding} = -37.29$ kJ·mol^{-1}) was more favored than that of Fx/2-HP-β-CD IC at molar ratio of 1:1 ($\Delta G_{binding} = -15.94$ kJ·mol^{-1}). It was illustrated that Fx and 2-HP-β-CD tend to form more stable inclusion complex with molar ratio of 1:2. There were some amends occurred in the geometrical structure of Fx to ensure the most stable inclusion complex, including bond angle, bond distance and dihedral angle amendment of the guest component [37]. It was observed that the hexatomic rings at either end of the long chain of Fx were embedded into the 2-HP-β-CD cavities in the optimized geometry (Fig. 5b). The hydrogen bondings (yellow dotted lines) between Fx and 2-HP-β-CD were the mainly intermolecular interactions present in the inclusion complex. These interactions between the host and guest molecules maintained the stability of the complexes, and the simulation results were consistent in the consequences of FT-IR characterization.

3.5. Solubilization of Fx/2-HP-β-CD IC

The water solubility of Fx/2-HP-β-CD IC was assessed by preparing
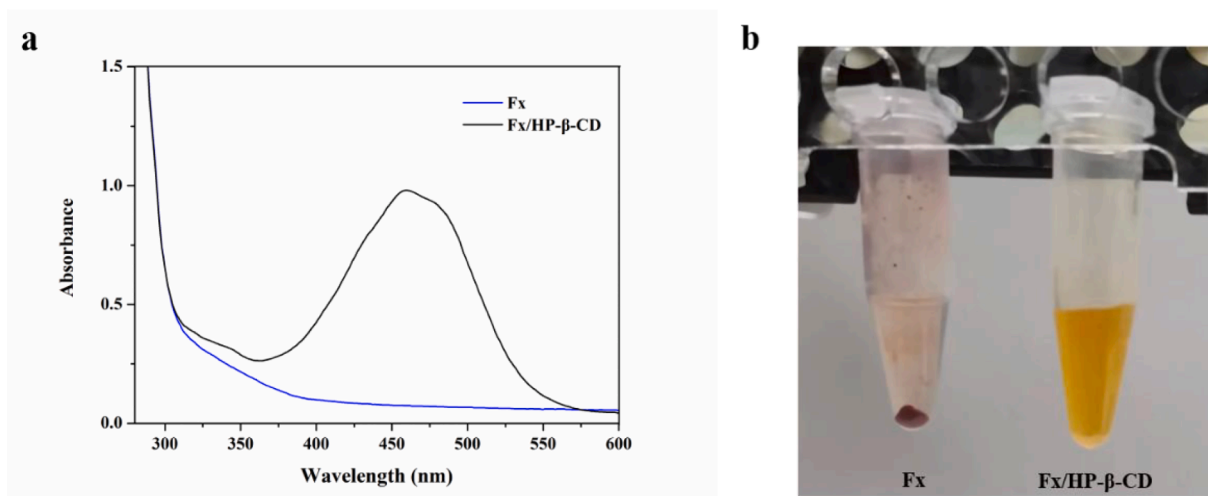

Fig. 6. Water solubility diagram of Fx and Fx/2-HP-β-CD IC having the same amount of Fx. (a) UV–Vis absorption spectra and (b) the dissolution behavior.
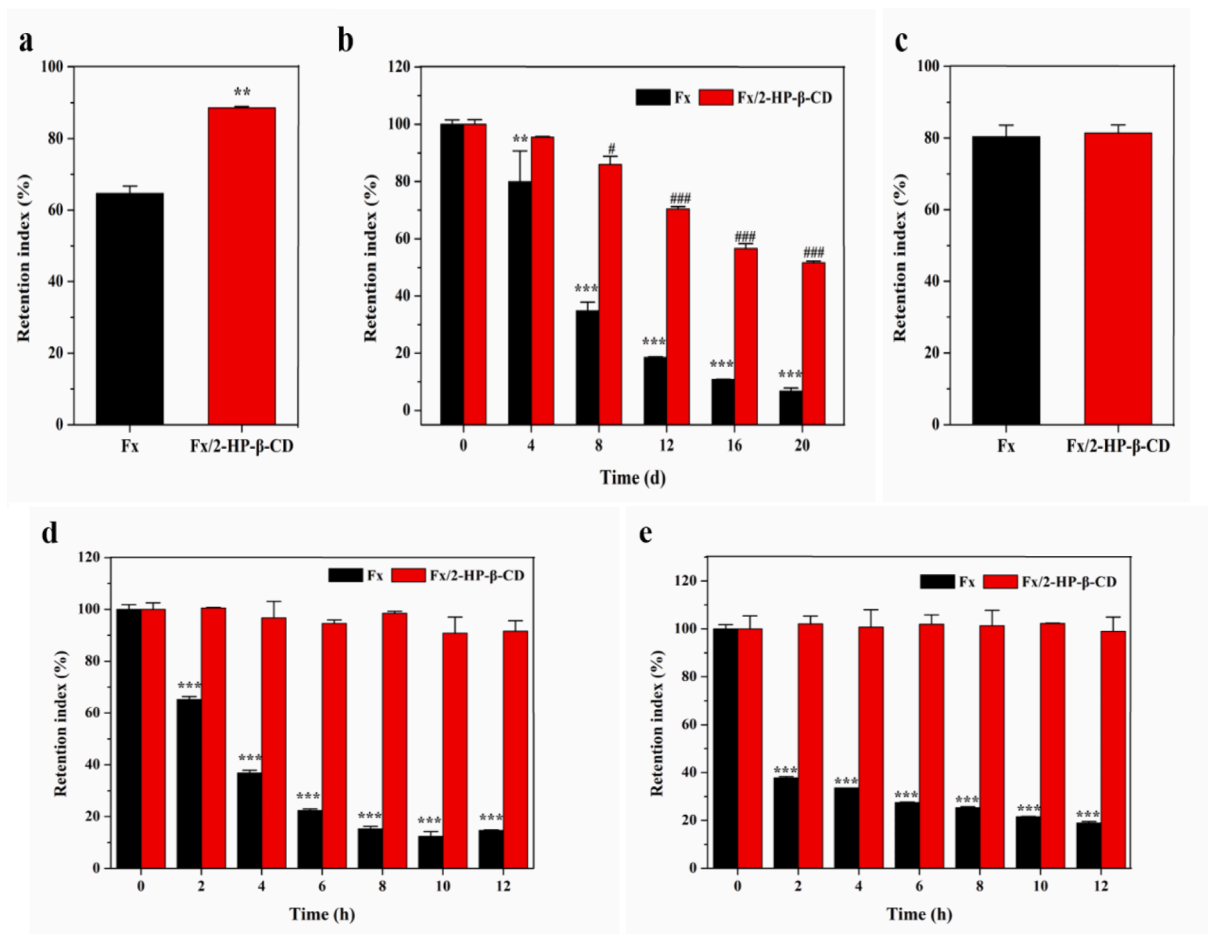
Fig. 7. The stability of Fx and Fx/2-HP-β-CD IC in different conditions: (a) pasteurization, (b) 25 °C storage, (c) simulating gastric fluid, (d) simulating intestinal fluid, and (e) physiological salt solution.

the saturated solution. As evident from Fig. 6, Fx exhibited a remarkable increment of solubility in water after complexation by 2-HP-β-CD, increasing from 0.05 μg/mL to 151.12 μg/mL. As described above, Fx is a nearly water-insoluble compound. The water solubility of Fx increased about 3,022 times by complexing with 2-HP-β-CD. In a study of red bell pepper carotenoids/2-HP-β-CD inclusion complexes, the water-solubility properties of complex samples increased 660 times compared with the crude pigments [38]. In some other studies, 2-HP-β-CD was also reported to be able to formulate inclusion complex with hydrophobic compounds and thus enhance their solubility in water [20,39]. Therefore, we conclude that 2-HP-β-CD was an effective novel delivery for Fx by forming complex, which could be beneficial to expand the applicability of Fx in pharmaceutical and dietary supplements.

3.6. Heat, Storage, and gastrointestinal stability of Fx/2-HP-β-CD IC

Fx is known to be easily degraded when exposed to high temperature, oxygen and physiological microenvironments, which may be a limit to the application of Fx-contained products [19,40]. In this study, the chemical stability of Fx/2-HP-β-CD IC in simulated processing and storage stage was evaluated according to the retention rate of Fx under pasteurization and long-time storage conditions. As shown in Fig. 7a, <65 % of the free Fx was retained after pasteurization treatment (65 °C, 30 min), whereas nearly 90 % of Fx encapsulated in Fx/2-HP-β-CD IC was reserved over the same period. In the storage stability test, the Fx/2-HP-β-CD IC still retained 51.6 % of the initial content of Fx after stored at 25 °C for 20 d, while the free Fx degraded a lot, with only 6.8 % of Fx left (Fig. 7b). All the results indicated that complexation with 2-HP-β-CD

provided a better protective effect on Fx against heat and long-time storage.

Subsequently, the chemical stability of Fx/2-HP-β-CD IC was evaluated under mimic internal environmental conditions. The retention index of Fx was about 80 % in free Fx and Fx/2-HP-β-CD IC after they were incubated in basic simulated stomach pH solution (pH = 2.0 HCl) at 37 °C for 30 min (Fig. 7c), which indicated that complexation by 2-HP-β-CD had no effect on the gastric stability of Fx. However, by complexing with 2-HP-β-CD significantly improved the chemical stability of Fx in basic simulated small intestinal fluid (pH = 7.4 PBS), with greater than 90 % Fx remained after incubated at 37 °C for 12 h (Fig. 7d). Obviously, complexation with 2-HP-β-CD in protecting Fx from the simulated small intestinal fluid was more effective than the gastric fluid. In addition, complexation with 2-HP-β-CD also improved the chemical stability of Fx in basic physiological environment and there was almost no change in the content of Fx throughout the whole 12 h incubation (Fig. 7e). The chemical stability of Fx was greatly improved after complexation with 2-HP-β-CD under basic simulated small intestinal and physiological environments, which suggested that complexation with 2-HP-β-CD may be an effective measure to deliver Fx through gastrointestinal tract and realize a high bioavailibility.

3.7. Antiproliferative activity against tumor cell lines

Fx has been proven to have antiproliferative and apoptosis-inducing effects on human colorectal carcinoma (CRC) cells [41–43]. In current study, the antiproliferative activity of Fx/2-HP-β-CD IC was assayed on CRC cell lines, HCT116 and Caco-2, by MTT assay. Free Fx at

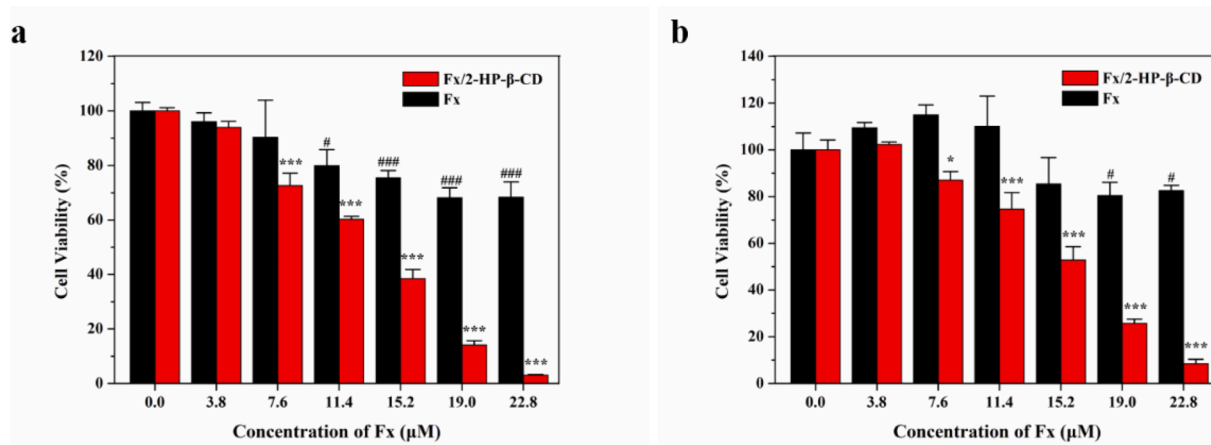**Fig. 8.** Cell proliferative inhibitory effects of Fx and Fx/2-HP-β-CD IC on (a) HCT116 cell and (b) Caco-2 cell. Data were expressed as the mean ± SD. Significant differences ($^{\#}$, *$p < 0.05$; ***$p < 0.001$) compared to respective control.

concentrations of 11.4 μM and 19.0 μM initiated to reduce the viability of HCT116 and Caco-2 cells after 24 h treatment, respectively (Fig. 8). Other study also reported that 5 μM or 10 μM Fx reduced the viability of HCT116 more intensively than that of Caco-2 cells after 72 h treatment [43]. Free Fx at 50 μM significantly reduced HCT116 cell viability up to 95 %, while the combination of Fx (10 μM) and 5-Fu (1 or 10 μM) also generated a distinct inhibition effect on cell viability (nealy 40 % or 75 %) [44]. Fx/2-HP-β-CD IC exerted significant antiproliferative effects on both cell lines in a dose-dependent manner. Complexed Fx at the concentrations higher than 7.6 μM reduced the viability of HCT116 and Caco-2 cells more intensively than free Fx with homologous concentrations ($p < 0.05$). The corresponding IC$_{50}$ values of complexed Fx were measured as 12.0 μM, 14.86 μM towards HCT116 and Caco-2 cells, respectively (Fig. S1). In order to eliminate the intervention effect of 2-HP-β-CD, we also include it as a control and no effect on cell proliferation was observed (Fig. S2). Therefore, we reasonably speculated that Fx/2-HP-β-CD IC may be an effective delivery system which could improve the solubility, stability of Fx thus increase the infusion of Fx into CRC cells and facilitate stronger antitumor activity.

4. Conclusion

In this study, Fx/2-HP-β-CD IC was prepared assisted by ultrasound method, and then characterized by phase-solubility, UV–Vis, SEM, FT-IR, XRD and DSC. Fx molecules entered into the hydrophobic cavities of 2-HP-β-CDs and formed more stable inclusion complex with 1:2 stoichiometric ratio through intermolecular interaction such as hydrogen bonds and hydrophobic interaction. The aqueous solubility and chemical stability against heat, storage, and physiological conditions were improved remarkably due to the formation of stable Fx/2-HP-β-CD IC. Meanwhile, the bioassay revealed that compared to free Fx, the Fx/2-HP-β-CD IC presented higher antitumor activity against HCT116 and Caco-2 cell lines. In summary, the formation of inclusion complex between Fx and 2-HP-β-CD was a promising technology to improve its water solubility, chemical stability and antitumor activity. The findings obtained in this study provide reliable information for Fx to be used in food and pharmaceutical industries by establishing delivery system of Fx/2-HP-β-CD IC.

Declaration of Competing Interest

The authors declare that they have no known competing financial interests or personal relationships that could have appeared to influence the work reported in this paper.

Data availability

Data will be made available on request.

Acknowledgements

Appendix A. Supplementary data

Supplementary data to this article can be found online at https://doi.org/10.1016/j.ultsonch.2022.106215.

References

[1] J. Peng, J.P. Yuan, C.F. Wu, J.H. Wang, Fucoxanthin, a marine carotenoid present in brown seaweeds and diatoms: metabolism and bioactivities relevant to human health, Mar. Drugs 9 (2011) 1806–1828.

[2] S.R. Kumar, M. Hosokawa, K. Miyashita, Fucoxanthin: a marine carotenoid exerting anti-cancer effects by affecting multiple mechanisms, Mar. Drugs 11 (2013) 5130–5147.

[3] A. Zarekarizi, L. Hoffmann, D. Burritt, Approaches for the sustainable production of fucoxanthin, a xanthophyll with potential health benefits, J. Appl. Phycol. 31 (2019) 281–299.

[4] H. Maeda, Nutraceutical effects of fucoxanthin for obesity and diabetes therapy: a review, J. Oleo Sci. (2015) ess14226.

[5] S. Mohamadnia, O. Tavakoli, M.A. Faramarzi, Z. Shamsollahi, Production of fucoxanthin by the microalga Tisochrysis lutea: a review of recent developments, Aquaculture 516 (2020), 734637.

[6] T. Hashimoto, Y. Ozaki, M. Mizuno, M. Yoshida, Y. Nishitani, T. Azuma, A. Komoto, T. Maoka, Y. Tanino, K. Kanazawa, Pharmacokinetics of fucoxanthinol in human plasma after the oral administration of kombu extract, Br. J. Nutr. 107 (2012) 1566–1569.

[7] J. Zhu, X. Sun, S. Wang, Y. Xu, D. Wang, Formation of nanocomplexes comprising whey proteins and fucoxanthin: characterization, spectroscopic analysis, and molecular docking, Food Hydrocolloid. 63 (2017) 391–403.

[8] S.M. Badr-Eldin, S.A. Elkheshen, M.M. Ghorab, Inclusion complexes of tadalafil with natural and chemically modified β-cyclodextrins. I: preparation and *in-vitro* evaluation, Eur. J. Pharm. Biopharm. 70 (2008) 819–827.

[9] T.A. Nguyen, B. Liu, J. Zhao, D.S. Thomas, J.M. Hook, An investigation into the supramolecular structure, solubility, stability and antioxidant activity of rutin/cyclodextrin inclusion complex, Food Chem. 136 (2013) 186–192.

[10] N.E. Polyakov, T.V. Leshina, T.A. Konovalova, E.O. Hand, L.D. Kispert, Inclusion complexes of carotenoids with cyclodextrins: 1HNMR, EPR, and optical studies, Free Radic. Biol. Med. 36 (2004) 872–880.

[11] J. Wang, Y. Cao, B. Sun, C. Wang, Physicochemical and release characterisation of garlic oil-β-cyclodextrin inclusion complexes, Food Chem. 127 (2011) 1680–1685.

[12] J. Li, H. Xiao, J. Li, Y. Zhong, Drug carrier systems based on water-soluble cationic β-cyclodextrin polymers, Int. J. Pharm. 278 (2004) 329–342.

[13] Y. Ohtani, T. Irie, K. Uekama, K. Fukunaga, J. Pitha, Differential effects of α-, β-and γ-cyclodextrins on human erythrocytes, Eur. J. Biochem. 186 (1989) 17–22.

[14] S. Gould, R.C. Scott, 2-Hydroxypropyl-β-cyclodextrin (HP-β-CD): a toxicology review, Food Chem. Toxicol. 43 (2005) 1451–1459.

[15] T. Loftsson, D. Duchêne, Cyclodextrins and their pharmaceutical applications, Int. J. Pharm. 329 (2007) 1–11.

[16] S. Jiang, T. Zhao, Y. Wei, Z. Cao, Y. Xu, J. Wei, F. Xu, H. Wang, X. Shao, Preparation and characterization of tea tree oil/hydroxypropyl-β-cyclodextrin inclusion complex and its application to control brown rot in peach fruit, Food Hydrocolloid. 121 (2021), 107037.

[17] D.R. de Araujo, S.S. Tsuneda, C.M. Cereda, F.D.G. Carvalho, P.S. Preté, S. A. Fernandes, F. Yokaichiya, M.K. Franco, I. Mazzaro, L.F. Fraceto, Development and pharmacological evaluation of ropivacaine-2-hydroxypropyl-β-cyclodextrin inclusion complex, Eur. J. Pharm. Sci. 33 (2008) 60–71.

[18] I.M. Cavalcanti, E.A. Mendonça, M.C. Lira, S.B. Honrato, C.A. Camara, R. V. Amorim, J. Mendes Filho, M.M. Rabello, M.Z. Hernandes, A.P. Ayala, The encapsulation of β-lapachone in 2-hydroxypropyl-β-cyclodextrin inclusion complex into liposomes: a physicochemical evaluation and molecular modeling approach, Eur. J. Pharm. Sci. 44 (2011) 332–340.

[19] X. Sun, Y. Xu, L. Zhao, H. Yan, S. Wang, D. Wang, The stability and bioaccessibility of fucoxanthin in spray-dried microcapsules based on various biopolymers, RSC Adv. 8 (2018) 35139–35149.

[20] H. Cui, S. Siva, L. Lin, Ultrasound processed cuminaldehyde/2-hydroxypropyl-β-cyclodextrin inclusion complex: preparation, characterization and antibacterial activity, Ultrason. Sonochem. 56 (2019) 84–93.

[21] T. Higuchi, K.A. Connors, Phase solubility studies, Adv. Anal. Chem. Instrum. 117–212 (1965).

[22] H.A. Benesi, J. Hildebrand, A spectrophotometric investigation of the interaction of iodine with aromatic hydrocarbons, J. Am. Chem. Soc. 71 (1949) 2703–2707.

[23] C. Liu, Z. Liu, X. Sun, S. Zhang, S. Wang, F. Feng, D. Wang, Y. Xu, Fabrication and characterization of β-lactoglobulin-based nanocomplexes composed of chitosan oligosaccharides as vehicles for delivery of astaxanthin, J. Agric. Food Chem. 66 (2018) 6717–6726.

[24] P. Michalska, A. Wojnicz, A. Ruiz-Nuño, S. Abril, I. Buendia, R. León, Inclusion complex of ITH12674 with 2-hydroxypropyl-β-cyclodextrin: preparation, physical characterization and pharmacological effect, Carbohydr. Polym. 157 (2017) 94–104.

[25] L. Yuan, S. Li, D. Huo, W. Zhou, X. Wang, D. Bai, J. Hu, Studies on the preparation and photostability of avobenzone and (2-hydroxy) propyl-β-cyclodextrin inclusion complex, J. Photochem. Photobiol. A: Chem. 369 (2019) 174–180.

[26] J. Zhu, C. Wang, J. Gao, H. Wu, Q. Sun, Aggregation of fucoxanthin and its effects on binding and delivery properties of whey proteins, J. Agric. Food Chem. 67 (2019) 10412–10422.

[27] M.A. Minhas, A. Rauf, S. Rauf, F.T. Minhas, N. Memon, A. Jabbar, M.I. Bhanger, M. I. Malik, Selective and efficient extraction of cationic dyes from industrial effluents through polymer inclusion membrane, Sep. Purif. Technol. 272 (2021), 118883.

[28] X. Qiao, L. Yang, X. Hu, Y. Cao, Z. Li, J. Xu, C. Xue, Characterization and evaluation of inclusion complexes between astaxanthin esters with different molecular

[29] structures and hydroxypropyl-β-cyclodextrin, Food Hydrocolloid. 110 (2021), 106208.

[29] H. Li, Y. Xu, X. Sun, S. Wang, J. Wang, J. Zhu, D. Wang, L. Zhao, Stability, bioactivity, and bioaccessibility of fucoxanthin in zein-caseinate composite nanoparticles fabricated at neutral pH by antisolvent precipitation, Food Hydrocolloid. 84 (2018) 379–388.

[30] R. Bonnett, A. Mallams, A. Spark, J. Tee, B. Weedon, A. McCormick, Carotenoids and related compounds. Part XX. Structure and reactions of fucoxanthin, J. Chem. Soc. C (1969) 429–454.

[31] B. dos Santos Lima, C. de Alcântara Campos, A.C.R. da Silva Santos, V.C.N. Santos, G.d.G.G. Trindade, S. Shanmugam, E.W.M. Pereira, R.N. Marreto, M.C. Duarte, J.R. G. da Silva Almeida, Development of morin/hydroxypropyl-β-cyclodextrin inclusion complex: enhancement of bioavailability, antihyperalgesic and anti-inflammatory effects, Food Chem. Toxicol. 126 (2019) 15–24.

[32] L.J. Yang, S.H. Wang, S.Y. Zhou, F. Zhao, Q. Chang, M.Y. Li, W. Chen, X.D. Yang, Supramolecular system of podophyllotoxin and hydroxypropyl-β-cyclodextrin: characterization, inclusion mode, docking calculation, solubilization, stability and cytotoxic activity, Mater. Sci. Eng., C 76 (2017) 1136–1145.

[33] M.M. Meier, M.T. Luiz, B. Szpoganicz, V. Soldi, Thermal analysis behavior of β-and γ-cyclodextrin inclusion complexes with capric and caprilic acid, Thermochim. Acta 375 (2001) 153–160.

[34] A.R. Hedges, Industrial applications of cyclodextrins, Chem. Rev. 98 (1998) 2035–2044.

[35] B. Liu, W. Li, T.A. Nguyen, J. Zhao, Empirical, thermodynamic and quantum-chemical investigations of inclusion complexation between flavanones and (2-hydroxypropyl)-cyclodextrins, Food Chem. 134 (2012) 926–932.

[36] N. Rajendiran, S. Siva, Inclusion complex of sulfadimethoxine with cyclodextrins: preparation and characterization, Carbohydr. Polym. 101 (2014) 828–836.

[37] S. Siva, S.K. Nayaki, N. Rajendiran, Spectral and molecular modeling investigations of supramolecular complexes of mefenamic acid and aceclofenac with α-and β-cyclodextrin, Spectrochim. Acta, Part A 174 (2017) 349–362.

[38] N. de Lima Petito, D. da Silva Dias, V.G. Costa, D.Q. Falcão, K.G. de Lima Araujo, Increasing solubility of red bell pepper carotenoids by complexation with 2-hydroxypropyl-β-cyclodextrin, Food Chem. 208 (2016) 124–131.

[39] A. Celebioglu, T. Uyar, Fast-dissolving antioxidant curcumin/cyclodextrin inclusion complex electrospun nanofibrous webs, Food Chem. 317 (2020), 126397.

[40] I.-K. Mok, J.-R. Yoon, C.-H. Pan, S.M. Kim, Development, quantification, method validation, and stability study of a novel fucoxanthin-fortified milk, J. Agric. Food Chem. 64 (2016) 6196–6202.

[41] M. Hosokawa, M. Kudo, H. Maeda, H. Kohno, T. Tanaka, K. Miyashita, Fucoxanthin induces apoptosis and enhances the antiproliferative effect of the PPARγ ligand, troglitazone, on colon cancer cells, BBA-Gen. Subjects 1675 (2004) 113–119.

[42] S. Zorofchian Moghadamtousi, H. Karimian, R. Khanabdali, M. Razavi, M. Firoozinia, K. Zandi, H. Abdul Kadir, Anticancer and antitumor potential of fucoidan and fucoxanthin, two main metabolites isolated from brown algae, Sci. World J. 2014 (2014), 768323.

[43] E. Kotake-Nara, T. Sugawara, A. Nagao, Antiproliferative effect of neoxanthin and fucoxanthin on cultured cells, Fish. Sci. 71 (2005) 459–461.

[44] E. Lopes-Costa, M. Abreu, D. Gargiulo, E. Rocha, A.A. Ramos, Anticancer effects of seaweed compounds fucoxanthin and phloroglucinol, alone and in combination with 5-fluorouracil in colon cells, J. Toxicol. Environ. Health, Part A 80 (2017) 776–787.